Analytical Modelling of Sound Transmission Through a Row of Thick-walled Channels

Mohcene Oulmi, Michel Roger, Benali Boualem

ANALYTICAL MODELLING OF SOUND TRANSMISSION THROUGH A ROW OF THICK-WALLED CHANNELS

Mohcene Oulmi[1,2] **Michel Roger**[1] **Benali Boualem**[2]
[1] Laboratoire de Mécanique des Fluides et d'Acoustique, École Centrale de Lyon , France
[2] Alstom, 7 avenue de Lattre de Tassigny - BP 49, 25290 Ornans, France
mohcene.oulmi@ec-lyon.fr

ABSTRACT

The present work is dealing with the transmission of oblique plane waves through a periodic row of thick-walled channels of finite length. It is aimed at investigating how sound is transmitted in some parts of the ventilation ducts integrated in electrical machines used in railways applications.

A two-dimensional analytical mode-matching method without flow is proposed, according to which modal expressions are written in sub-domains and matched according to conservation laws of fluid dynamics. The transmission and reflection coefficients are computed from the matching equations. Effects of channel length, frequency, wall thickness, are discussed. A particular attention is paid to the resonances in the system.

1. INTRODUCTION

The reduction of the noise generated by electrical machines used in railway traction has become a very important criterion during their design phase. The noise comes from three main sources, of vibrational, aerodynamic and electromagnetic origins. Among these contributions, aerodynamic noise is dominant at high rotation speeds. It is generated by the ventilation system of the machines. The latter consists of several elements: radial impeller, guide vanes and cooling channels. More precisely the noise generated by the impingement of the impeller wakes on the guide vanes is transmitted through all components of the ventilation system. It is therefore important to be able to predict the sound propagation in the ventilation system at the early design stage in order to avoid any resonance that can amplify the noise.

The analytical methods are better suited at this stage due to the very low computational time compared to numerical simulations.

In a complicate architecture various analytical models of noise propagation must be set up as a successive combination of sub-models. After having split the complete geometry into simplified blocks form mathematical tractability. The present work is dealing only with the problem of noise transmission through the cooling channels. The typical configuration is illustrated in Fig.1. It features two thin annular parts connected to a periodic array of channels, the interfaces including both the channel ends and rigid front walls. At most frequencies of interest the annulus thickness and the channel cross-section are smaller than wavelengths, which justifies that a $2D$ approach is selected to investigate primary technological effects. For this an unwrapped cylindrical cut of the true geometry is described in Cartesian coordinates. The radial impeller and the guide vanes located upstream of the left-side annulus are ignored but they generate sound that is considered as incident plane waves on the system.

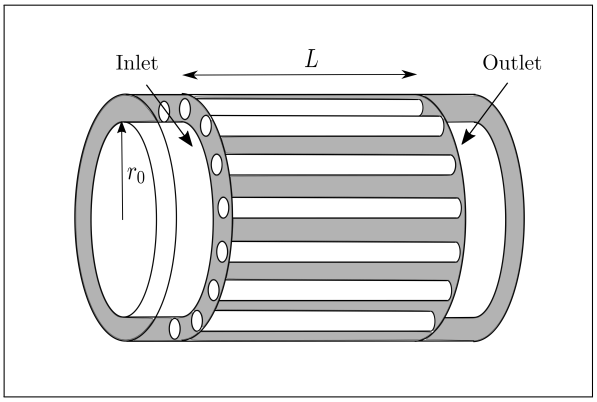

Figure 1: A typical configuration of the ventilation ducts of electrical machines

Several studies on sound transmission in acoustic waveguide discontinuities have been suggested in literature [1–4]. These models are valid only when two segments of different properties are connected to each other. In our case the channels are periodically excited in the same way as a row of outlet guide vanes of axial-flow turbomachines. Thus why a $2D$ mode-matching technique previously applied to model rotor-stator stages has been selected.

The simplicity of the present paper is to consider the transmission of oblique plane waves through a row of thick-walled channels. The mode matching technique is presented in detail in section 2. The results and the influence of physical parameters on sound propagation are shown in section 3.

2. MODE MATCHING METHOD

The mode-matching method is usually applied to deal with problems of transmission of waves at an interface, which

includes electromagnetic [5] and acoustic waves [6–9]. It is applied in the frequency domain on the Helmholtz equation. it allows calculating the modal amplitudes of reflected and transmitted waves. This technique is usable when the geometry can be considered as the junction of several sub-domains. The unwrapped representation of a cylindrical cut of the ventilation ducts at the radius r_0 is shown in Fig.2. The channel walls have a thickness b and are assumed to be perfectly rigid. The channel width is $a = 2\pi r_0/B - b$, B being the number of channels.

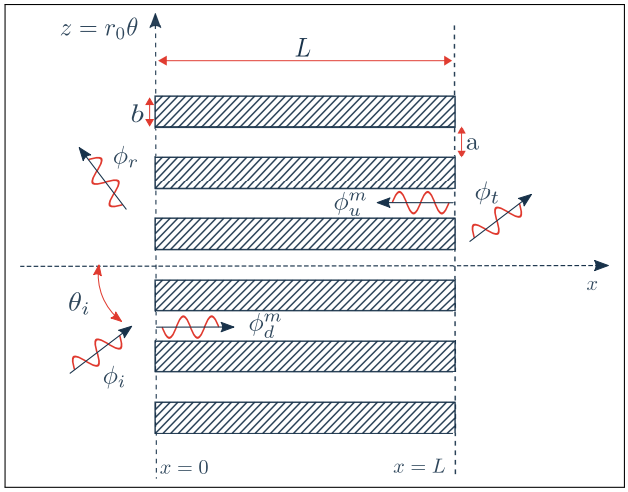

Figure 2: Two-dimensional unwrapped representation of the scattering of an acoustic wave through a row of thick-walled channels

The incident wave of potential ϕ_i is scattered at the interface $x = 0$ and generates reflected waves ϕ_r propagating upstream of the interface and transmitted waves ϕ_d into the channels. The latter propagate downstream to the open ends of channels $x = L$, generating a reflected field ϕ_u in the channels and a transmitted field ϕ_t downstream.

The mode matching technique is used in four steps:

- Dividing the geometry into sub-domains in which the Helmholtz equation is separable.
- Describing the sound field as a sum of orthogonal modes in each sub-domain.
- Matching the acoustic fields at each interface using the continuity of pressure and axial velocity.
- Solving the matching equations by matrix inversion to get the modal coefficients.

2.1 Acoustic Potentials

A time harmonic factor $\mathrm{e}^{-\mathrm{i}\omega t}$ is implicitly assumed throughout this paper. All the acoustic fields are described by their acoustic potentials. The Helmholtz equation is written as:

$$\frac{\partial^2\phi(x,z)}{\partial x^2} + \frac{\partial^2\phi(x,z)}{\partial z^2} + k^2\phi(x,z) = 0 \qquad (1)$$

where $k = \omega/c$ is the acoustic wavenumber, ω the angular frequency and c is the sound speed. This equation can be solved by separation of variables.

The acoustic pressure and axial velocity are related to the acoustic potential by the equations:

$$p = \mathrm{i}\omega\rho_0\phi \qquad (2)$$

$$v^x = \frac{\partial\phi}{\partial x} \qquad (3)$$

The incident field ϕ_i is considered as a plane wave propagating upstream of the interface $x = 0$, in the direction of the positive x with an angle θ_i. The potential of the incident wave is written as:

$$\phi_i(x,z) = \mathrm{e}^{\mathrm{i}\alpha_i z}\mathrm{e}^{\mathrm{i}k_i^+ x} \qquad (4)$$

with

$$\alpha_i = k\sin(\theta_i) = \frac{n}{r_0}, \quad k_i^+ = \sqrt{k^2 - \alpha_i^2}$$

n being the number of lobes.

The potential of the reflected wave reads

$$\phi_r(x,z) = \sum_{s=-\infty}^{+\infty} R_s\mathrm{e}^{\mathrm{i}\alpha_s z}\mathrm{e}^{\mathrm{i}k_s^- x} \qquad (5)$$

with

$$\alpha_s = \alpha_i + s\frac{2\pi}{a+b}, \quad k_s^- = -\sqrt{k^2 - \alpha_s^2}$$

The acoustic potential of the transmitted wave ϕ_d in the m^{th} channel is given by:

$$\phi_d^m(x,z) = \sum_{q=0}^{+\infty} D_q^0\mathrm{e}^{\mathrm{i}m\alpha_i(a+b)}\cos(\alpha_q\left[z - m(a+b)\right]) \times \mathrm{e}^{\mathrm{i}k_q^+ x} \qquad (6)$$

with

$$\alpha_q = q\frac{\pi}{a}, \quad k_q^+ = \sqrt{k^2 - \alpha_q^2}$$

where $\mathrm{e}^{\mathrm{i}m\alpha_i(a+b)}$ is the phase shift between adjacent channels.

The potential of the wave propagating upstream ϕ_u^m from the interface $x = L$ is expressed as

$$\phi_u^m(x,z) = \sum_{q=0}^{+\infty} U_q^0\mathrm{e}^{\mathrm{i}m\alpha_i(a+b)}\cos(\alpha_q\left[z - m(a+b)\right]) \times \mathrm{e}^{\mathrm{i}k_q^-(x-L)} \qquad (7)$$

with

$$k_q^- = -\sqrt{k^2 - \alpha_q^2}$$

The transmitted potential can be written as:

$$\phi_r(x,z) = \sum_{s=-\infty}^{+\infty} R_s\mathrm{e}^{\mathrm{i}\alpha_s z}\mathrm{e}^{\mathrm{i}k_s^- x} \qquad (8)$$

with

$$k_s^+ = \sqrt{k^2 - \alpha_s^2}$$

2.2 Matching equations

The only unknowns in this problem are the modal coefficients R_s, D_q, U_q and T_s. In order to calculate them, the mode matching technique must be applied on the both ends of the channels. The matching equations are obtained from the continuity of the acoustic pressure and the axial velocity at the open ends of channels. The acoustic pressure and the axial velocity are gathered into a vector Ξ

$$\Xi_g(x,z) = \begin{pmatrix} p_g(x,z) \\ \\ v_g^x(x,z) \end{pmatrix}, \quad g = \{i,r,d,u,t\} \tag{9}$$

The continuity of the acoustic pressure and axial velocity at the interfaces $x = 0$ and $x = L$ is written as

$$\Xi_i(0,z) + \Xi_r(0,z) = \Xi_d(0,z) + \Xi_u(0,z) \tag{10}$$

$$\Xi_d(L,z) + \Xi_u(L,z) = \Xi_t(L,z) \tag{11}$$

The rigid-wall boundary condition is imposed on the front face of the channel separators which corresponds to vanishing normal velocity $v^x = 0$. This condition is equivalent to

$$\int_0^{a+b} (v_i + v_r)\mathrm{e}^{-\mathrm{i}\alpha_\nu z}\mathrm{d}z = \int_0^{a} (v_i + v_r)\mathrm{e}^{-\mathrm{i}\alpha_\nu z}\mathrm{d}z \tag{12}$$

2.2.1 *Channel inlet* $(x = 0)$

After replacing the expressions of acoustic pressure and axial velocity in Eqn.(10), we obtain:

$$\sum_{s=-\infty}^{+\infty} (\delta_{s,0} + R_s)\,\mathrm{e}^{\mathrm{i}\alpha_s z} = \sum_{q=0}^{+\infty} \left(D_q^0 + U_q^0 \mathrm{e}^{-\mathrm{i}k_q^- L}\right) \times \cos(\alpha_q z) \tag{13}$$

$$\sum_{s=-\infty}^{+\infty} (R_s - \delta_{s,0})\,k_s^- \mathrm{e}^{\mathrm{i}\alpha_s z} = \sum_{q=0}^{+\infty} \left(D_q^0 - U_q^0 \mathrm{e}^{-\mathrm{i}k_q^- L}\right) \times k_q^+ \cos(\alpha_q z) \tag{14}$$

with

$$\delta_{s,0} = \begin{cases} 1 & ,\text{if } s = 0 \\ 0 & ,\text{if } s \neq 0 \end{cases}$$

A modal projection must be used to solve the system of equations, based on the orthogonality properties of the modes. The orthogonality relation is given by

$$\int_0^a \Psi_i \Psi_j^* \mathrm{d}z = 0, \quad \text{if} \quad i \neq j$$

where Ψ_j^* is the complex conjugate of the eigenfunction Ψ_i. The equations of continuity of acoustic pressure and axial velocity are projected on the eigenfunctions of the channels and of the unbounded medium respectively.

The modal projection for the pressure, leads to

$$\sum_{s=-\infty}^{+\infty} (\delta_{s,0} + R_s)\,\Lambda_{\mu,s} = \left(D_\mu^0 + U_\mu^0 \mathrm{e}^{-\mathrm{i}k_\mu^- L}\right) \times \frac{a}{2}(1 + \delta_{\mu,0}) \tag{15}$$

where

$$\alpha_\mu = \mu\frac{\pi}{a}$$

The matrix term $\Lambda_{\mu,s}$ is found analytically as:

$$\Lambda_{\mu,s} = \int_0^a \mathrm{e}^{\mathrm{i}\alpha_s z}\cos(\alpha_\mu z)\mathrm{d}z$$

$$\Lambda_{\mu,s} = \begin{cases} \frac{\mathrm{i}\alpha_s\left[1-(-1)^\mu \mathrm{e}^{-\mathrm{i}\alpha_s a}\right]}{\alpha_s^2 - \alpha_\mu^2} & ,\text{if } \alpha_\mu \neq \alpha_s \\ \\ \frac{a}{2}(1 + \delta_{\mu,0}) & ,\text{if } \alpha_\mu = \alpha_s \end{cases} \tag{16}$$

The projection of Eqn.(14) on the eigenfunction $\mathrm{e}^{-\mathrm{i}\alpha_\nu z}$ gives:

$$\int_0^a (v_i + v_r)\mathrm{e}^{-\mathrm{i}\alpha_\nu z}\mathrm{d}z = \int_0^a (v_q + v_u)\mathrm{e}^{-\mathrm{i}\alpha_\nu z}\mathrm{d}z \tag{17}$$

The Eqn.(17) and Eqn.(12) give

$$\int_0^{a+b} (v_i + v_r)\mathrm{e}^{-\mathrm{i}\alpha_\nu z}\mathrm{d}z = \int_0^a (v_q + v_u)\mathrm{e}^{-\mathrm{i}\alpha_\nu z}\mathrm{d}z \tag{18}$$

After accounting for the orthogonality, we obtain

$$(a+b)\,(R_\nu - \delta_{\nu,0})\,k_\nu^- = \sum_{q=0}^{+\infty} \left(D_q^0 - U_q^0 \mathrm{e}^{-\mathrm{i}k_q^- L}\right) \times k_q^+ \varphi_{\nu,q} \tag{19}$$

where

$$\alpha_\nu = \nu\frac{2\pi}{a+b}$$

and

$$\varphi_{\nu,q} = \int_0^a \cos(\alpha_q z)\mathrm{e}^{-\mathrm{i}\alpha_\nu z}\mathrm{d}z$$

$$\varphi_{\nu,q} = \begin{cases} \frac{\mathrm{i}\alpha_\nu\left[(-1)^q \mathrm{e}^{-\mathrm{i}\alpha_\nu a} - 1\right]}{\alpha_\nu^2 - \alpha_q^2} & ,\text{if } \alpha_q \neq \alpha_\nu \\ \\ \frac{a}{2}(1 + \delta_{q,0}) & ,\text{if } \alpha_q = \alpha_\nu \end{cases} \tag{20}$$

The Eqn.(15) and Eqn.(19) are valid for any mode, so that we can write in matrix notation:

$$\begin{cases} (\delta_0 + R)\,\underline{\Lambda} &=& D + \mathcal{U} \\ \\ (R - \delta_0) &=& (D - \mathcal{U})\,\underline{\varphi} \end{cases} \tag{21}$$

where

$$\underline{\varphi} = \frac{1}{(a+b)}\frac{k_q^+}{k_\nu^-}\varphi_{\nu,q} \quad ,\underline{\Lambda} = \frac{1}{\frac{a}{2}(1+\delta_{\mu,0})}\Lambda_{\mu,s}$$

$$\mathcal{U} = U_\mu^0 \mathrm{e}^{-\mathrm{i}k_\mu^- L}$$

Finally, the vector of reflection coefficients is given by

$$R = \left(\underline{I} - \underline{\varphi}\underline{\Lambda}\right)^{-1} \left[\left(\underline{I} + \underline{\varphi}\underline{\Lambda}\right)\delta_0 - 2\underline{\varphi}\mathcal{U}\right] \quad (22)$$

with I is the identity matrix.

The transmission coefficients are directly deduced from Eqn.(15) as:

$$D_\mu^0 = \frac{1}{\frac{a}{2}(1+\delta_{\mu,0})} \sum_{s=-\infty}^{+\infty} \left(\delta_{s,0} + R_s\right)\Lambda_{\mu,s} - U_\mu^0 \mathrm{e}^{-\mathrm{i}k_q^- L} \quad (23)$$

2.2.2 Channel outlet $(x = L)$

For the channel m = 0, the continuity equations at the interface $(x = L)$ are written

$$\sum_{q=0}^{+\infty} \left(D_q^0 \mathrm{e}^{\mathrm{i}k_q^+ L} + U_q^0\right)\cos(\alpha_q z) = \sum_{s=-\infty}^{+\infty} T_s \mathrm{e}^{\mathrm{i}\alpha_s z} \quad (24)$$

$$\sum_{q=0}^{+\infty} \left(U_q^0 - D_q^0 \mathrm{e}^{\mathrm{i}k_q^+ L}\right) k_q^- \cos(\alpha_q z) = \sum_{s=-\infty}^{+\infty} T_s k_s^+ \mathrm{e}^{\mathrm{i}\alpha_s z} \quad (25)$$

In the same way, we project the equations of acoustic pressure Eqn.(24) and axial velocity Eqn.(25) on the eigenfunctions $\cos(\alpha_\mu z)$ and $\mathrm{e}^{-\mathrm{i}\alpha_\nu z}$, respectively, and obtain:

$$\left(D_\mu^0 \mathrm{e}^{\mathrm{i}k_\mu^+ L} + U_\mu^0\right)\frac{a}{2}(1+\delta_{\mu,0}) = \sum_{s=-\infty}^{+\infty} T_s \Lambda_{\mu,s} \quad (26)$$

$$\sum_{q=0}^{+\infty} \left(U_q^0 - D_q^0 \mathrm{e}^{\mathrm{i}k_q^+ L}\right) k_q^- \varphi_{\nu,q} = (a+b) k_\nu^+ T_\nu \quad (27)$$

The matrix notation of Eqn.(26) and Eqn.(27) is :

$$\begin{cases} \mathcal{D} + U = T\underline{\Lambda} \\ (U - \mathcal{D})\,\underline{\varphi_2} = T \end{cases} \quad (28)$$

where

$$\underline{\varphi_2} = \frac{1}{(a+b)}\frac{k_q^-}{k_\nu^+}\varphi_{\nu,q} \quad , \mathcal{D} = D_\mu^0 \mathrm{e}^{\mathrm{i}k_\mu^+ L}.$$

The resolution of this equation by matrix inversion allows the determination of the vector of the reflection coefficients U.

$$U = \left(\underline{\Lambda}\underline{\varphi_2} - \underline{I}\right)^{-1}\left(\underline{\Lambda}\underline{\varphi_2} + \underline{I}\right)\mathcal{D} \quad (29)$$

Using Eqn.(27), the transmission coefficients are determined by:

$$T_\nu = \frac{1}{(a+b)} \sum_{q=0}^{+\infty} \left(U_q^0 - D_q^0 \mathrm{e}^{\mathrm{i}k_q^+ L}\right)\frac{k_q^-}{k_\nu^+}\varphi_{\nu,q} \quad (30)$$

2.3 Solving procedure

The two sets of equations are solved by an iterative procedure because of the multiple reflections inside the channels. The index of iterations used in the solving procedure is noted j. In the first iteration $j = 0$ we assume no reflected wave in the channels: $U_q^0 = 0$. The Eqn.(10) becomes:

$$\Xi_i(0,z) + \Xi_r^{j=1}(0,z) = \Xi_d^{j=1}(0,z) \quad (31)$$

The Eqn.(31) is used to compute the reflection coefficient R_s and the transmission coefficient D_q^0. The latter is used in Eqn.(32) to compute the new values of U_q^0 and T_s.

$$\Xi_d^{j=1}(L,z) + \Xi_u^{j=1}(L,z) = \Xi_t^{j=1}(L,z) \quad (32)$$

The Eqn.(33) is solved again using the new value of U_q^0 as input. The procedure is repeated till convergence. The different steps of the iterative method are shown in Fig.3.

$$\Xi_i(0,z) + \Xi_r^{j=2}(0,z) = \Xi_d^{j=2}(0,z) + \Xi_u^{j=1}(0,z) \quad (33)$$

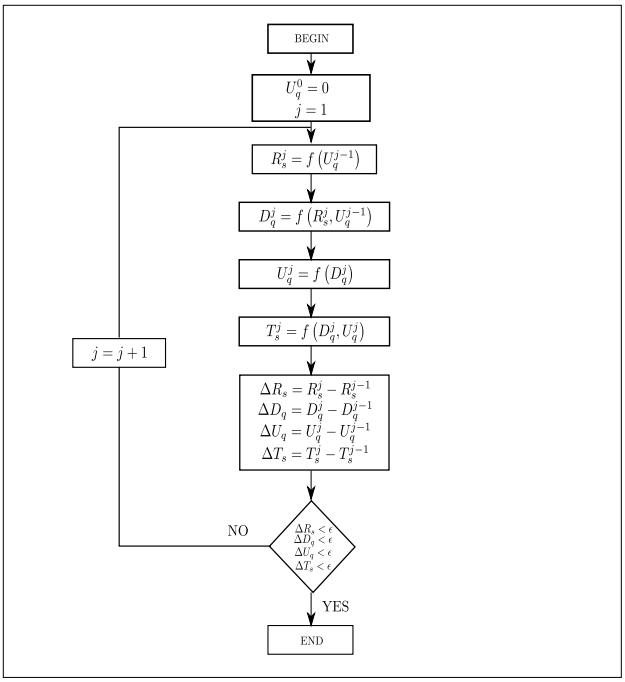

Figure 3: Solving procedure

In practice the infinite series must be truncated to have a finite number of modes. The maximum numbers of modes N_s and N_q depend on the number of cut-on modes, with $-N_s \leq s \leq N_s$ and $0 \leq q \leq N_q - 1$. The ratio $(2N_s + 1)/N_q$ must be close to $(a + b)/a$ to satisfy the edge condition at best. N_q is given by:

$$N_q \approx (2N_s + 1)\frac{a}{a+b}$$

3. RESULTS

The mode matching technique is applied in this section to a test case of 12 channels. The parameters are listed in Tab.1.

$f\ (Hz)$	$b\ (m)$	$r_0\ (m)$	$L\ (m)$	n
2800	0.04	0.15	0.3	3

Table 1: Test-case parameters

A convergence study on the number of iterations is carried out, by estimating that the results are converged when the relative variation of the modal amplitudes between successive iterations is less than 10^{-9}. The Fig.4 shows that convergence only requires a few iterations, about 12.

Fig.5 shows the instantaneous pressure field for the incident mode $n = 3$. Upstream of the interface $x = 0$, the acoustic field is dominated by the incident wave, modulated by the reflected wave. The latter propagates upstream of the interface as a specular reflection. Fig.6 presents the instantaneous pressure and velocity profiles along an axial line at center of the 6^{th} channel, showing the continuity of the physical quantities on both interfaces $x = 0$ and $x = L$.

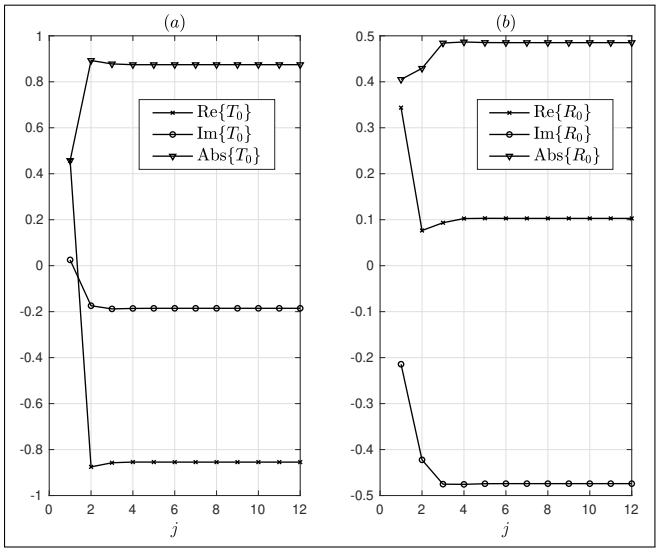

Figure 4: Modal amplitudes of the reflected R_s (a) and transmitted T_s (b) modes of order $s = 0$ as functions of the number of iterations.

The Fig.7 presents the modulus of the complex-valued modal coefficients of the acoustic fields. The blue and red bars denote cut-on and cut-off modes respectively. They indicate that only the modes of order s = 0 and q = 0 are cut-on and that therefore the reflected and transmitted fields only contain the incident mode order $n = 3$. The other modes are cut off, attenuated exponentially on both sides of the interfaces, they do not participate in acoustic radiation. However taking the evanescent modes into account is very important to ensure the continuity of the acoustic field at the interfaces and to accurately calculate the amplitudes of the cut-on modes.

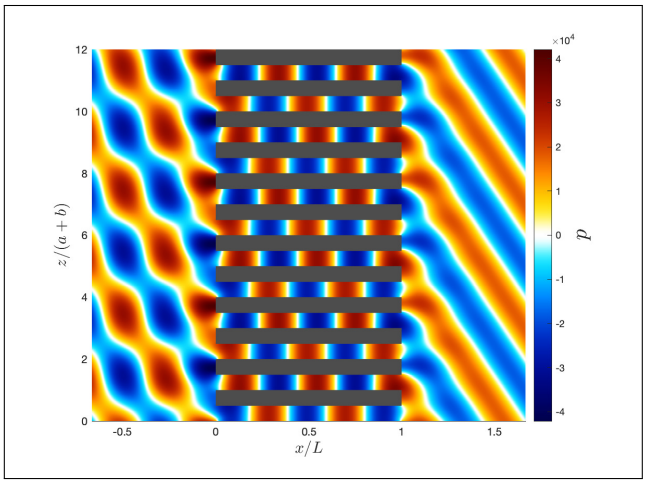

Figure 5: Typical instantaneous acoustic pressure field. Incident mode $n = 3$.

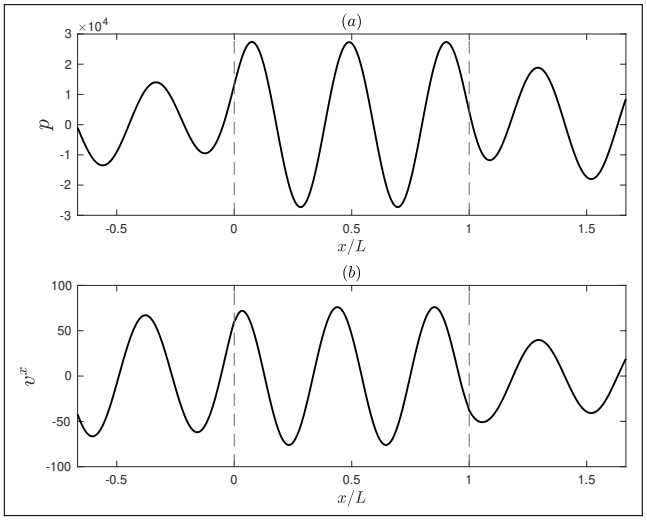

Figure 6: Instantaneous acoustic pressure (a), and velocity (b) profiles from Fig.5. $z = 6(a + b) + a/2$.

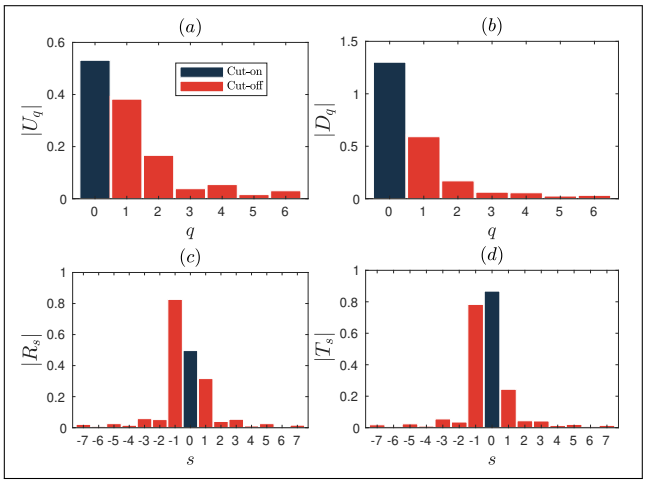

Figure 7: Modulus of the modal coefficients from the test case in Fig.5

3.1 Effect of frequency

The effect of frequency on the acoustic field is discussed in this section and the reflected $\mathcal{P}_r$ and transmitted $\mathcal{P}_t$ acous-

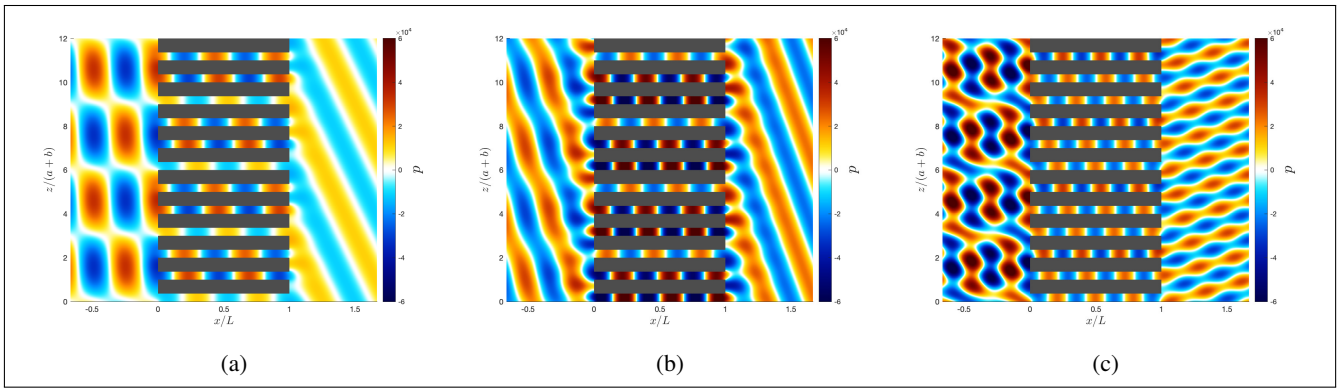

Figure 8: Instantaneous acoustic pressure fields for various frequencies. (a) $f = 2500$ Hz. (b) $f = 3225$ Hz. (c) $f = 4000$ Hz. Incident mode $n = 2$, $b = 0.05$m, $a = 0.028$m.

tic powers are plotted as function of frequency in Fig.9 for the incident mode $n = 2$. The Fig.8 shows the instantaneous sound pressure fields for three different frequencies. When the incident wave propagates through a channel, the reflected and transmitted modes of order 2 (for $s = 0$) are always cut-on. The cut-off frequency is defined as the minimum frequency f_c below which only the mode $s = 0$ is cut-on. For the configuration studied, this cut-off frequency is 3683 Hz.

In low frequency for $f < f_c$ (Figs. 8b and 8a), the transmitted power is maximum at resonance frequencies while the reflected power is extremely low.

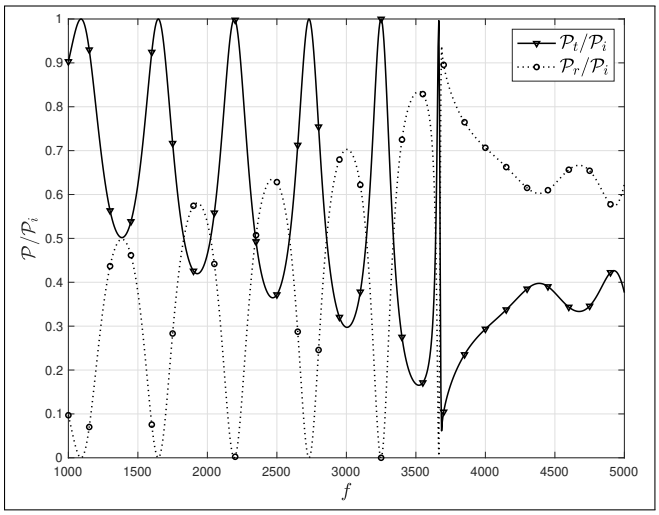

Figure 9: Variations of the transmitted P_t and reflected P_r acoustic powers the frequency

Acoustic resonance are expected *a priori* when the length of the channels L is a multiple of the half wavelength $\lambda/2$. But for open pipes of transverse dimension much smaller than the wavelength, an effective length larger than the true length must be considered. The resonant frequencies are obtained as

$$f_{n_r} = \frac{n_r c_0}{2L_e}$$

with

$$L_e = L + L_{corr}$$

where L_{corr} accounts for the end corrections, which correspond to equivalent reflecting points just outside the channels [10].

When the frequency exceeds the cutoff frequency f_c, a second mode becomes cut-on, as illustrated in Fig.8c. The interference pattern becomes more complex upstream of the channels, and the acoustic energy is distributed differently between the upstream and downstream fields.

3.2 Effect of Thickness

One of the most important aspects in this study is the influence of the wall thickness b on sound transmission. The Fig.10 shows the instantaneous acoustic pressure fields for various wall thicknesses.

Fig.10a confirms that a small thickness generally yields only small reflections. As thickness increases, the reflection becomes more important as shown in Fig. 10b. In the case of very thick walls Fig.10c the incident wave is strongly reflected by the front surfaces, causing more interference than in other cases.

4. CONCLUSION

An analytical model of sound transmission through a periodic row of thick-walled channels has been proposed in this paper in order to model the propagation of noise in some parts of ventilation ducts used in electrical machines. The mode-matching technique allowed us to compute the modal amplitudes of the transmission and reflection coefficients. The matching equations based on the continuity of the acoustic pressure and axial velocity were written at both channel ends. An iterative method has been proposed to take into account the multiple reflections at these ends. The convergence of the calculation was reached after few iterations.

The results have shown that the distribution of the acoustic power is highly dependent on the frequency. The incident wave is completely transmitted when its frequency is equal to a resonant frequency of the channels.

A parametric study on the influence of wall thickness on propagation of the acoustic waves has shown that the

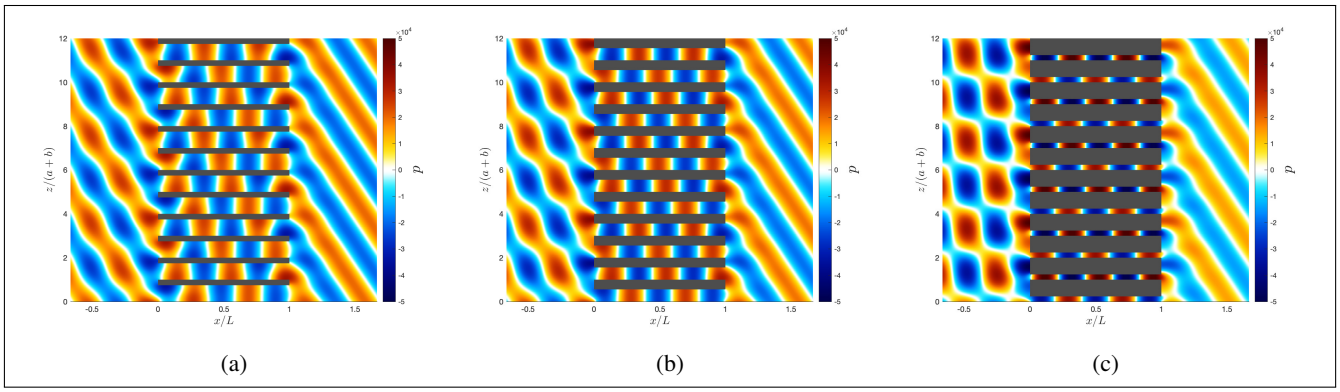

Figure 10: Instantaneous acoustic pressure fields for various thickness values . (a) $b = 0.02$ m. (b) $b = 0.035$ m. (c) $b = 0.06$ m. Incident mode $n = 3$, $f = 2800$ Hz.

reflected field upstream of the channels increases with wall thickness.

5. ACKNOWLEDGMENTS

This work was performed within the framework of the LABEX CeLyA (ANR-10-LABX-0060) of Université de Lyon, within the program "Investissements d'Avenir" (ANR-11-IDEX-0007) operated by the French National Research Agency (ANR).

6. REFERENCES

[1] D. Homentcovschi and R. N. Miles, "A re-expansion method for determining the acoustical impedance and the scattering matrix for the waveguide discontinuity problem," *The Journal of the Acoustical Society of America*, vol. 128, no. 2, pp. 628–638, 2010.

[2] R. Alfredson, "The propagation of sound in a circular duct of continuously varying cross-sectional area," *Journal of Sound and Vibration*, vol. 23, no. 4, pp. 433 – 442, 1972.

[3] A.Roure, "Propagation du son dans des conduits à section continûment variable," *Marseille. Euromech 94*, Septembre 1977.

[4] S. Rienstra and A. Hirschberg, *An introduction to acoustics*. IWDE report, Technische Universiteit Eindhoven, 2001.

[5] R. Mittra and S. Lee, *Analytical techniques in the theory of guided waves*. Macmillan series in electrical science, Macmillan, 1971.

[6] J. Ingenito and M. Roger, "Analytical modelling of sound transmission through the passage of centrifugal compressors," in *13th AIAA/CEAS Aeroacoustics Conference*, 2007.

[7] M. Roger, "Analytical modelling of wake-interaction noise in centrifugal compressors with vaned diffuser," in *10th AIAA/CEAS Aeroacoustics Conference*, 2004.

[8] S. Bouley, B. François, M. Roger, H. Posson, and S. Moreau, "On a two-dimensional mode-matching technique for sound generation and transmission in axial-flow outlet guide vanes," *Journal of Sound and Vibration*, vol. 403, pp. 190 – 213, 2017.

[9] M. Roger, S. Moreau, and A. Marsan, "Generation and transmission of spiral acoustic waves in multi-stage subsonic radial compressors," in *20th AIAA/CEAS Aeroacoustics Conference*, 2014.

[10] Y. Ando, "On the sound radiation from semi-infinite circular pipe of certain wall thickness," *Acustica*, vol. 22, pp. 219 – 225, 1969.